1 Binary Collisions

1.1 Lab System

Momentum Conservation:

$$M_1 v_{1,0} = M_1 v_{1,f} cos\theta_1 + M_2 v_{2,f} cos\theta_2$$

Max Energy Transfer/Head on Collision

$$T_2^{max} = \frac{4M_1 M_2}{(M_1 + M_2)^2} T_0 = \Lambda T_0$$

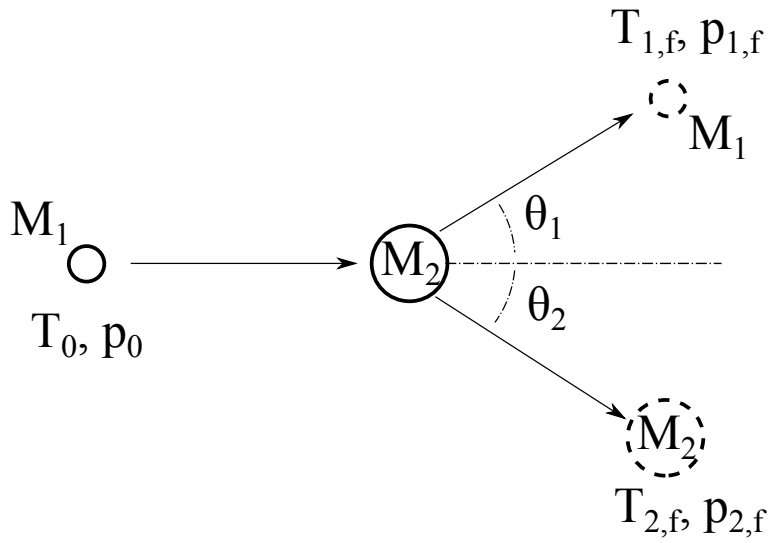

Figure 1: Lab System Collision Diagram

1.2 Center of Mass System

Momentum Conservation:

$$v_{cm} = \frac{v_1 M_1 + v_2 M_2}{M_1 + M_2}$$

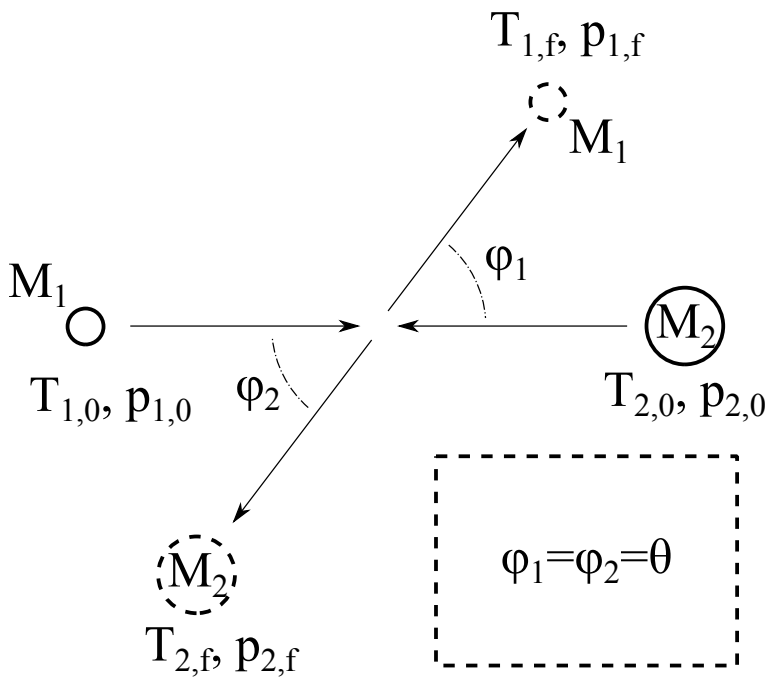

Figure 2: Center of Mass System Collision Diagram

1.3 Lab System and Center of Mass System Compared

Comparison between angles:

$$tan\theta_1 = \frac{\frac{M_2}{M_1} sin\theta}{1 + \frac{M_2}{M_1} cos\theta}$$

Comparison between energies:

$$E_{2,f} = \Lambda E_{1,0} sin^2 \frac{\theta}{2}$$

$$E_{1,f} = E_{1,0} - E_{2,f}$$

2 Potentials

Table 1: Comparison of Potential Interactions

Name	Expression	Verbal	Energy Range
Electrostatic (Coulomb)	$V(r) = \frac{Z_1 Z_2 e^2}{r}$ $e^2 = 14.4eV \cdot \breve{A}$	only potential between nuclei	$100keV \rightarrow MeV$
Closed Shell (Screened Coulomb)	$V(r) = \frac{Z_1 Z_2 a}{r} e^{\frac{-r}{a}}$ $a = \frac{\sqrt{2}\lambda a_B}{(Z_1^{2/3} + Z_2^{2/3})^{1/2}}$ $a_B = 0.53\breve{A}$ $\lambda \approx 1$	shells overlap and must move to a higher shell	$1keV \rightarrow 100keV$
Born-Meyer	$V(r) = e^{\frac{-r}{\rho}}$	repulsion from electrons forced into unoccupied states	$eV \rightarrow 1keV$
Thomas-Fermi Potential	$V(r) = \frac{Z_1 Z_2 e^2}{r} \chi(\frac{r}{a})$ $\chi(\frac{r}{a}) = 0.35e^{\frac{-0.3r}{a}} + 0.55e^{\frac{-1.2r}{a}} + 0.10e^{\frac{-6.0r}{a}}$	assumes electrons form ideal gas filling potential well about positive charged core	intermediate E

3 Cross Sections

3.1 Differential Cross Sections

Generalized Isotropic:

$$\sigma_s(E_i) = \int_0^{\pi} \sigma_s(E_i, \theta) \cdot 2\pi \cdot sin\theta d\theta$$

Hard Sphere:

$$\sigma(E,T) = \frac{C}{E}$$
$$C = \pi \frac{M_1}{M_2} \cdot \frac{Z_1^2 Z_2^2 e^4}{1}$$

Coulomb:

$$\sigma(E,T) = \frac{C}{ET^2} = \pi Z_1^2 Z_2^2 e^4 \cdot \frac{M_1}{M_2} \cdot \frac{1}{ET^2}$$

Inverse Square:

$$\sigma(E,T) = \frac{C}{E^{1/2}T^{3/2}} = \pi Z_1^2 Z_2^2 e^4 \cdot \frac{M_1}{M_2} \cdot \frac{1}{E^{1/2}T^{3/2}}$$

Born-Meyer:

$$\sigma(E,T) = \frac{\pi B^2}{\Lambda E} \left[ln(\frac{A}{\xi E}) \right]^2$$
$$\Lambda = \frac{4M_1 M_2}{(M_1 + M_2)}$$
$$\xi = \frac{M_2}{M_1 + M_2}$$

4 Energy Loss

4.1 Production Rate

$$Rate = N\int_0^\infty\int_0^\infty \Phi(E)\sigma_d(E,T)dEdT$$

4.2 Energy Loss Mechanisms

Mean Distance between Collisions:

$$\lambda = \frac{1}{N\sigma}$$

$$\frac{dE}{dx} = \frac{\overline{T}}{\lambda} = \frac{\frac{\int T\sigma(E,T)dt}{\int \sigma(E,T)dT}}{\frac{1}{\int \sigma(E,T)dT}} = N\int T\sigma(E,T)dT$$

Weighted Average Recoil Spectra: (fraction of recoil ions below a certain energy)

$$W(T) = \frac{\int_{E_d}^{T} T\sigma(E,T)dT}{\int_{E_d}^{\Lambda E} T\sigma(E,T)dT} = \frac{ln(T) - ln(E_d)}{ln(\Lambda E) - ln(E_d)}$$

4.3 Nuclear Stopping

Using Coulomb potential:

$$\sigma_s(E,T) = \frac{\pi b_0^2}{4}\left(\frac{\Lambda E}{T^2}\right)$$

$$b_0 = \frac{Z_1 Z_2 e^2}{\xi E}$$

$$\xi = \frac{M_2}{M_1 + M_2}$$

$$\left.\frac{dE}{dx}\right|_n = NS_n(E) = N\int T\sigma(E,T)dT = N\int_{T_{min}}^{T_{max}} T\frac{\pi b_0^2}{4}\left(\frac{\Lambda E}{T^2}\right)dT$$

$$T_{max} = \Lambda E$$

$$T_{min} = E_a = \frac{Z_1 Z_2 e^2}{a}\left(\frac{M_1 + M_2}{M_2}\right)e^{-1}$$

$$a = screening\ radius = \frac{\sqrt{2}\lambda a_B}{(Z_1^{2/3} + Z_2^{2/3})^{1/2}}$$

$$\left.\frac{dE}{dx}\right|_n = N\pi\frac{Z_1^2 Z_2^2 e^4 M_1}{E_1 M_2} ln\frac{\Lambda E_1}{E_a}$$

Using Inverse Square Potential:

$$\left.\frac{dE}{dx}\right|_n = \frac{\pi^2}{4}Na^2\Lambda E_a$$

4.4 Electronic Stopping

High Energy:

$$\sigma(E,T) = \frac{\pi b_0^2}{4} \cdot \frac{\Lambda E}{T^2}$$

$$\left.\frac{dE}{dx}\right|_e N\pi \frac{Z_1^2 e^4 M_1}{E_1 M_e} ln \frac{4M_e E_1}{I M_1}$$

Low Energy (Lindhard):

$$\left.\frac{dE}{dx}\right|_e = \kappa\sqrt{E_1} \quad for\ 0 < E(keV) < 37Z^{7/3}$$

$$\kappa = 0.3NZ^{2/3}\frac{ev^{1/2}}{\breve{A}}$$

Minimum Ion Energy to release an electron

$$E_c = \frac{M_1}{4m_e} I$$

4.5 Electronic Stopping Power

Bethe Non-Relativistic

$$E > E_T \quad E_T = (24.8keV)A_1 Z_1^{4/3}$$

$$\frac{dE}{dx} = 2\pi N (Z_1^*)^2 Z_2 e^4 \frac{M_1}{E_1 m_e} ln\left(\frac{4m_e E_1}{I M_1}\right)$$

$$Z_1^* = \frac{Z_1^{1/3}\bar{h}}{e^2}\sqrt{\frac{2E_1}{M_1}}$$

Medium Energy

$$E_T > E > E_c \quad E_c = A$$

$$\frac{dE}{dx} = 0.4NZ_1^{2/3} Z_2 e^4 ln\left(\frac{4m_e E_1}{I M_1}\right)$$

Low Energy

$$E_c > E$$

$$\frac{dE}{dx} = \frac{0.3Z_1^{5/6} Z_2}{(Z_1^{2/3} + Z_2^{2/3})^{3/2}} \cdot \frac{N}{\sqrt{M_1}}\sqrt{E_1} \quad in\ \frac{eV}{\breve{A}}$$

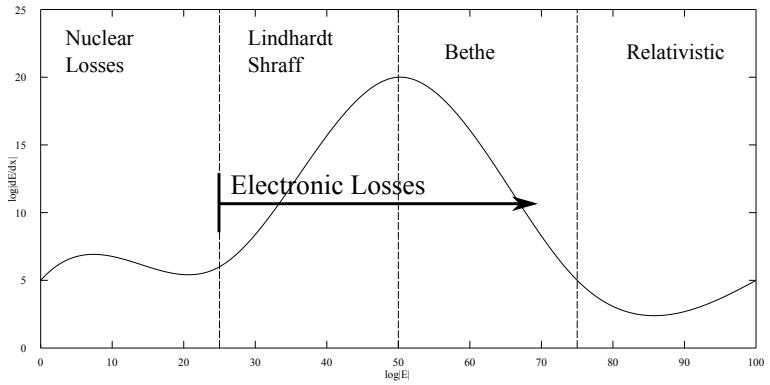

Figure 3: Electronic Stopping Power Plot

5 Ion Range and Range Distribution

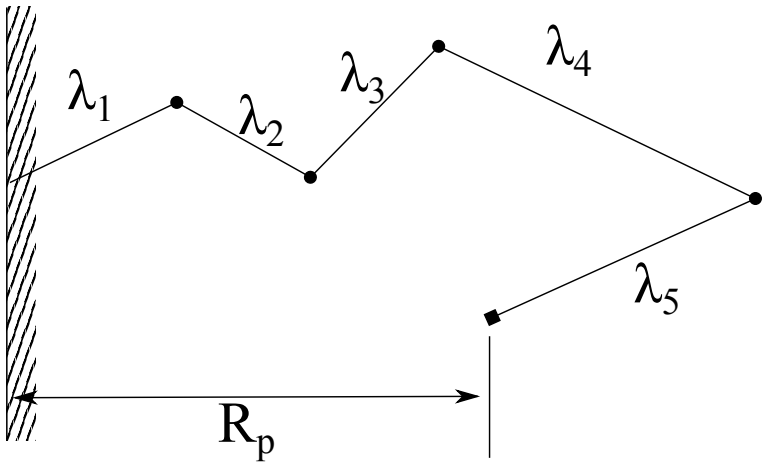

Figure 4: Projected Range Diagram

Moments:
1st Moment, Average:

$$\mu = \int x f(x) dx$$

2nd Moment, Variance:

$$\sigma^2 = \int (x-\mu)^2 f(x) dx$$

$$stdev = \sqrt{\sigma^2}$$

The range is defined by

$$R = \int_{E_0}^{0} \frac{dE}{dE/dx} = \int_{E_0}^{0} \frac{dE}{NS(E)}$$

$$R \approx \frac{R}{1+(M_2/3M_1)} \quad for\ similar\ mass\ \Delta R_p \approx 0.4 R_p \approx \frac{1.1}{2.5}\sqrt{\Lambda} R_p$$

6 Displacements

6.1 Definitions

- Displacement - lattice atom knocked from its lattice site
- Displacement per atom - average number of lattice displacements per lattice atom
- Primary Knock-on Atom - lattice atom displaced by incident particle
- Secondary Knock-on Atom - lattice atom displaced by PKA
- Displacement Rate (R_d) - displacements per unit volume per unit time
- Displacement Energy (E_d) - energy needed to displace an atom
- Range Straggling - the width vs depth ratio of the incoming ion based on relative mass of ion and substrate
- Displacement damage function ($\nu(T)$) - # of displaced atoms produced by a PKA with energy T

6.2 Displacement Energy

(emperical correlation)

$$E_d \approx 175 k_b T_{melt}$$

$$k_b = 1.38 \times 10^{-23} \frac{m^2 kg}{s^2 K} = 8.62 \times 10^{-5} \frac{eV}{K}$$

Kinchin-Pease Model for Displacement

- assumes collisions between like atoms
- hard sphere cross sections
- only nuclear stopping
- binary collision ignores binding energy
- crystal structure neglected

Hard Sphere Cross Section

$$\sigma(E,T) = \frac{\sigma_p}{\Lambda E}$$

K-P Displacement Damage Function

$$V(T) = \begin{cases} 0 & T \leq E_d \\ 1 & E_d \leq T < 2E_d \\ \frac{T}{2E_d} & 2E_d \leq T < E_c \\ \frac{E_c}{2E_d} & T \geq E_c \end{cases}$$

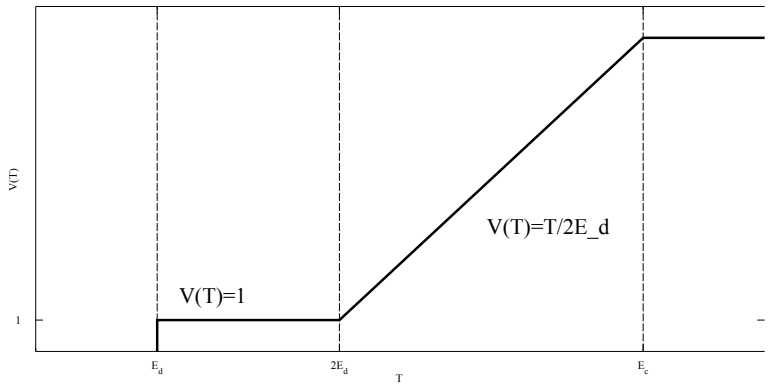

Figure 5: K-P Displacement Damage Graph

Removing the Hard Sphere assumption
Power Law:

$$V(T) = 0.57\frac{T}{2E_d}$$

Use Hard Sphere but remove E_c assumption

$$V(T) = \frac{T}{2E_d}\left(1 - \frac{4k}{\sigma N\sqrt{2E_d}}\right)$$

Comprehensive model with real potential and electronic stopping

$$V(T) = \xi(T)\left(\frac{T}{2E_d}\right)$$
$$\xi(T) = \frac{1}{(1 + 0.13(3.4\varepsilon^{1/6} + 0.4\varepsilon^{3/4} + \varepsilon))}$$
$$\varepsilon = \frac{Ea}{2Z^2e^2}$$
$$a = \frac{0.88a_B}{Z^{1/3}}$$
$$a_B = 0.053\,nm$$

Displacement Rate

$$R_d = N\int_0^\infty \Phi(E)\int_{E_d}^{\Lambda E} V(T)\sigma(E,T)dTdE$$

Reaction Rate

$$R_{PKA} = N\int_0^\infty \Phi(E)\sigma(E,T)dE$$

Displacement Cross Section:

$$\sigma_d(E_n) = \frac{\sigma_{el}(E_n)}{\Lambda E_n}\int_{E_d}^{\Lambda E_n}\left[1 + a_1(E_n)\cdot\left(1 - \frac{2E}{\Lambda E_n}\right)\right]V(E)dE + \frac{\sigma_{in}(E_n)}{\left(1 - \frac{(1+A)Q}{AE_n}\right)^{1/2}\Lambda E_n}\cdot\int_{E_{min}}^{E_{max}} V(E)dE$$

By ignoring inelastic scattering and only taking a_0 (isotropic scattering):

$$\sigma_d(E_n) = \left(\frac{\Lambda E_n}{4E_d}\right)\sigma_{el}(E_n)$$

7 Channeling and Focusing

7.1 Focusing

- Focusing refers to transfer of energy between atoms by nearly head on collisions along a row of atoms.

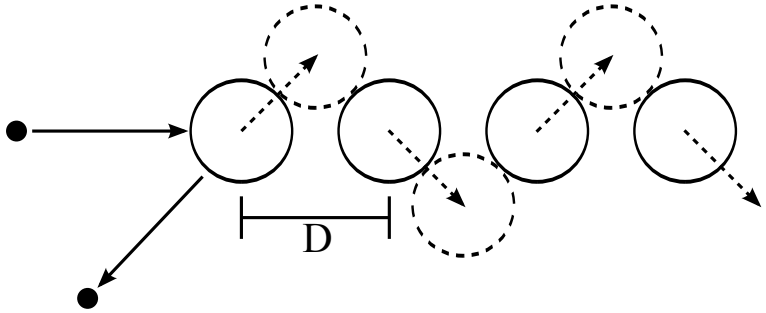

Figure 6: Focusing Diagram

- Focusing occurs only within certain energy limits:

$$E < E_{foc}$$

$$E_{foc} = 2V\frac{D}{2}$$

- Angles must be small enough to keep collisions in a line.
- A long series of head on collisions can transfer the kinetic energy down the row displacing all of the atoms by one lattice site.
- A vacancy is left at the beginning and an interstitial at the end.
- Long range focusing of a single atom is called a dynamic crowdion.
- Focusing chaings are terminated by lattice imprections such as
  - thermal vibrations
  - impurity atoms
  - dislocations
- If collision energy is less than replacement energy E_R, only energy transfer, not atom transfer.

7.2 Channeling

- Channeling is complementary process where atoms move long distances along open directions in the crystal structure.
- Atoms are channeled by glancing collisions with the atomic rows that act as walls.
- Ion emains in channel by low angle scattering and slows down mostly by electric stopping.
- In a uniform lattic a channeled ion follows simple harmonic motion with an energy dependent wavelength.
- As the channeled ion slows the probability of wide angle scatter increases, eventually causing termination of channeling.
- The channeling effect reduces the number of displacements created by an incoming particle
  - Example: a channeling probability of $P = 7\%$ in Fe with a $10\,keV$ PKA reduces displacements by 50%.

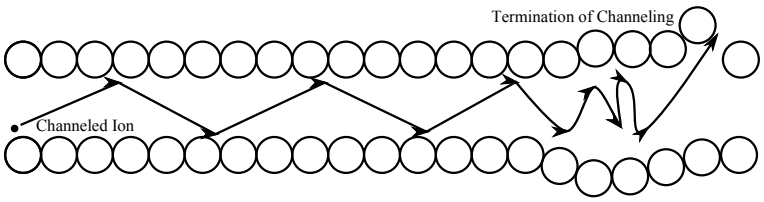

Figure 7: Channeling Diagram

8 Neutron Damage Mechanisms

8.1 Elastic Scattering

Elastic Scattering causes neutron damage if neutron energy

$$E > \frac{E_d}{\Lambda} \; for \; \Lambda = \frac{4A}{(1+A^2)}$$

- below $\sim 0.1\, MeV$ elastic scattering is isotropic
- above $\sim 0.1\, MeV$ elastic scattering exhibits a forward bias

elastic displacement cross section:

$$\sigma_{d_{el}}(E_n) = \int_{E_d}^{\Lambda E} \sigma_{el}(E_n, E)\nu(E)dE$$

$$\sigma_{el}(E_n, \theta) = \frac{\sigma_{el}(E_n)}{4\pi}(1 + a_1(E_n)cos\theta)$$

$$\left|\frac{a \cdot cos\theta}{dE}\right| = \frac{2}{\Lambda E_n}$$

8.2 Inelastic Scattering

Inelastic scatterin creates recoil nucleus after neutron emission

- Inelastic scattering occurs when compound nucleus is formed and neutron is re-emitted with less energy due to nuclear excitation (Q).
- Inelastic scattering is isotropic.
- The recoil energy after inelastic scattering is given by:

$$E = \frac{1}{2}\Lambda E_n \left[1 - \frac{(1+A)Q}{2AE_n} - \left(1 - \frac{(1+A)Q}{AE_n}\right)^{1/2} cos\theta\right]$$

Angular Cross Section:

$$\sigma_{in}(E_n, \theta) = \frac{\sigma_{in}(E_n)}{4\pi}$$

Angle to Energy transformation

$$\left|\frac{dcos\theta}{dE}\right|_{in} = \frac{2}{\Lambda E_{in}}\left[1 - \frac{(1+A)Q}{AE_n}\right]^{-1/2}$$

8.3 Recoils from (n, γ)

- Absorption of thermal neutrons and resulting photon release causes low energy recoil atoms.
- The recoil energy for heavy nuclei after photon emission is:

$$T \approx \frac{34}{A}\, keV$$

- (n, γ) recoils are significant contributors to damage in thermal reactors.

8.4 Damage Functions

To relate neutron exposure to macroscopic changes, semi-empirical damage functions have been created:

$$\Delta P_i = \Phi t \cdot \frac{\int G_i(E_n)\phi(E_n)dE_n}{\int \phi(E_n)dE_n}$$

9 Sputtering

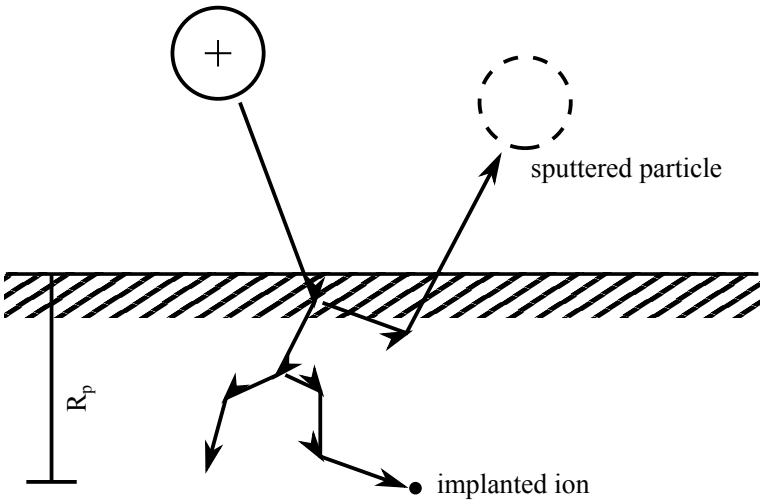

Figure 8: Sputtering Diagram

Suppering is the erosion of a material by energetic particles
Sputtering Yield

$$Y = sputtering\, yield = \frac{mean\, \#\, of\, emitted\, atoms}{incident\, particles}$$

for a medium mass ion in keV energies, typical values for Y are $\approx 1 \to 10$

$$Y = \gamma F_D(E_0)$$

$$\gamma = materials\, factor = \frac{4.2}{NU_0}$$

$$F_D(E_0) = \left.\frac{dE}{dx}\right|_{nuclear\, processes} = \alpha N S_n(E_0)$$

Matsunami Semi-Empirical Sputtering Formula

$$Y_E(E) = 0.42 \frac{\alpha_s Q_s S_n(E)}{U_0[1 + 0.35 U_0 S_e(\varepsilon)]} \left[1 + \left(\frac{E_{th}}{E}\right)^{1/2}\right]^{2.8}$$

$$E_{th} = \begin{cases} (\frac{4}{3})^6 \frac{U_0}{\Lambda} & M_1 \geq M_2 \\ \left(\frac{2M_1+2M_2}{M_1+M_2}\right)^6 \frac{U_0}{\Lambda} & M_1 < M_2 \end{cases}$$

$$S_n(E) = K_n S_n(\varepsilon)$$

$$K_n = \frac{8.478 Z_1 Z_2}{(Z_1^{2/3} + Z_2^{2/3})^{1/2}} \cdot \frac{M_1}{(M_1 + M_2)} \left(10^{-15} \frac{eV \cdot cm^2}{atom}\right)$$

$$S_n(\varepsilon) = \frac{3.441 \varepsilon^{1/2} ln(\varepsilon + 2.718)}{1 + 6.355\varepsilon^{1/2} + \varepsilon(6.882\varepsilon^{1/2} - 1.708)}$$

$$\varepsilon = \frac{0.03255}{Z_1 Z_2 (Z_1^{2/3} + Z_2^{2/3})^{1/2}} \cdot \frac{M_2}{(M_1 + M_2)} E\ (eV)$$

$$\alpha_s = 0.10 + 0.155 \left(\frac{M_2}{M_1}\right)^{0.73} + 0.001 \left(\frac{M_2}{M_1}\right)^{1.5}$$

9.1 Steady State Concentration during Ion Implantation

- Overtime the process of sputtering and implantation comes to equilibrium when the implanted ions are sputtered as fast as they are implanted.
- The distribution of implanted ion density is highest at the surface and decreases deeper into the material.
- if ion A is implanted into material B:

$$\frac{J_A}{J_B} = r \frac{N_B}{N_A}$$

$$r = \frac{probability\, of\, B\, atom\, sputtering}{probability\, of\, A\, atom\, sputtering}$$

- Define flux of incident ions as J_i

$$(J_A + J_B) = Y J_i$$

at steady state

$$J_A = J_i + J_B = (Y - 1)J$$

gives

$$\frac{(Y-1)J_i}{J_i} = r\frac{N_B}{N_A} \therefore \frac{N_A}{N_B} = \frac{r}{Y-1}$$

- Sputtering in Alloys and Compounds: elements in alloys will not be sputtered at equal rates because of binding energy and ejection probability.
- Preferntial Sputtering: for a homogenous sample with componentes A and B, surface conenctration N^s and bulk concentration N^B.

Initial Condition

$$\frac{N_A^s}{N_B^s} = \frac{N_A^B}{N_B^B}$$

Partial Yield

$$Y_A = \frac{ejected\, A}{incident}$$

and same for B.

$$\frac{Y_A}{Y_B} = r\frac{N^s A}{N^s B} \; for\, r\, typically\, between\, 0.5\, and\, 2$$

at $t = 0$

$$\frac{Y_A(0)}{Y_B(0)} = r\frac{N_A^s(0)}{N_B^s(0)} = r\frac{N_A^B}{N_B^B}$$

at $t = \infty$

$$\frac{Y_A(\infty)}{Y_B(\infty)} = \frac{N_A^B}{N_B^B}$$

at $t = \infty$, the surface becomes enriched with one element

$$\frac{N_A^s(\infty)}{N_B^s(\infty)} = \frac{1}{r}\frac{N_A^B}{N_B^B}$$

High Ion Dose Implantation

$$R_p\frac{dN_a}{dt} = J_i - J_A$$

- Max concentration is given by the reciprocal of the sputtering yields.
- Max concentration is obtained after sputtering of a thickness comparable with R_p.
- the amount of material sputtered

$$f = implantation\, layer\, thickness = \frac{Y\Phi_A}{N_0 R_p}$$

10 Point Defect Formation and Reaction Rates

10.1 Mechanisms of Diffusion

- Echarge and ring = swapping of lattice sites
- Vacancy is the most common
- Interstitial - moving between interstitial sites, only occurs when $r_{inter} < r_{atom}$
- Interstitialey - displacement of an atom into interstitial site
- Crowdion - atom added to lattice row but not in interstitial

10.2 Vacancy and Intersitial Movement

- Vacancies have a low formation energy and high migration energy so they are in higher concentrations than interstitials
- Vacancy loops are easily formed
- intersititals have higher formation energy and low migration energy making them more mobile than vacancies.

10.3 Point Defect Balance Equations

$$\frac{\partial C_v}{\partial t} = K_0 - K_{iv}C_iC_v - K_{vs}C_vC_s$$

$$\frac{\partial C_i}{\partial t} = K_0 - K_{iv}C_iC_v - K_{is}C_iC_s$$

$$K_{iv} = 4\pi r_{iv}(D_i + D_v)$$

$$K_{is} = 4\pi r_{is}D_i$$

$$K_{vs} = 4\pi r_{vs}D_v$$

Low Temp, Low Sink Density
Initially no losses and a linear increase

$$C_i = C_v = C$$

$$\frac{\partial C}{\partial t} = K_0$$

$$C = K_0 t$$

After some time τ_1, concentrations level off and quasi-steady state exists

$$C_i = C_v = C$$

$$\frac{\partial C}{\partial t} = k_0 - K_{iv}C^2 = 0$$

$$C = \left(\frac{K_0}{K_{iv}}\right)^{1/2}$$

to find τ_1

$$\left(\frac{K_0}{K_{iv}}\right)^{1/2} = K_0 t$$

$$t = \tau_1 = \left(\frac{1}{K_0 K_{iv}}\right)^{1/2}$$

During quasi-steady state, intersitital sare migrating faster than vacancies. Once interstitials start to reach sinks at τ_2 interstitials start to disappear and vacancies increase.

$$C_i = \left(\frac{K_0}{K_{iv}K_{is}C_s t}\right)^{1/2}$$

$$C_v = \left(\frac{K_0 K_{is} C_s t}{K_{iv}}\right)^{1/2}$$

at τ_2

$$\left(\frac{K_0}{K_{iv}}\right)^{1/2} = \left(\frac{K_0}{K_{iv}K_{is}C_s t}\right)^{1/2}$$

$$t = \frac{1}{K_{is}C_s} = \tau_2$$

at some time later τ_3 vacancies get to sinks causing C_i and C_r to level off and come to steady state

$$\frac{\partial C_v}{\partial t} = 0 = K_0 - K_{iv}C_iC_v - K_{vs}C_vC_s$$

at steady state $K_{vs}C_V = K_{is}C_i$

$$C_i = \frac{K_{vs}C_v}{K_{is}}$$

$$C_v = \left(\frac{K_0K_{is}}{K_{iv}K_{vs}} + \frac{K_{is}^2C_s^2}{4K_{iv}^2}\right)^{1/2} - \frac{K_{is}C_s}{2K_{iv}} \approx \left(\frac{K_0K_{is}}{K_{iv}K_{vs}}\right)^{1/2}$$

$$C_i = \left(\frac{K_0K_{vs}}{K_{iv}K_{vs}} + \frac{K_{vs}^2C_s^2}{4K_{iv}^2}\right)^{1/2} - \frac{K_{vs}C_s}{2K_{is}} \approx \left(\frac{K_0K_{vs}}{K_{iv}K_{is}}\right)^{1/2}$$

to find τ_3

$$\tau_3 = \frac{1}{K_{vs}C_s}$$

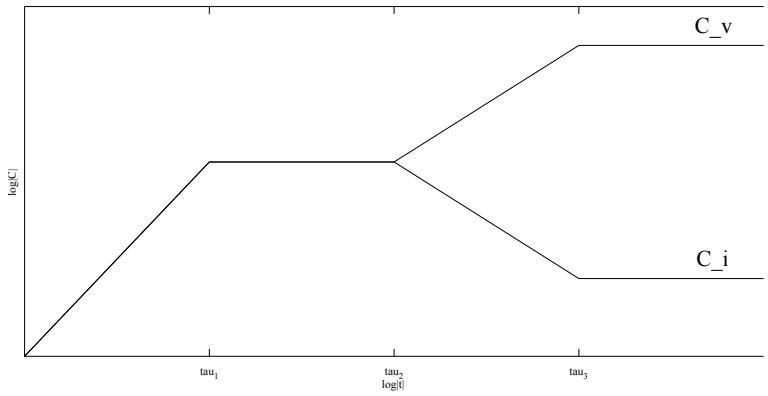

Figure 9: Low Temp Low Sink Density Plot

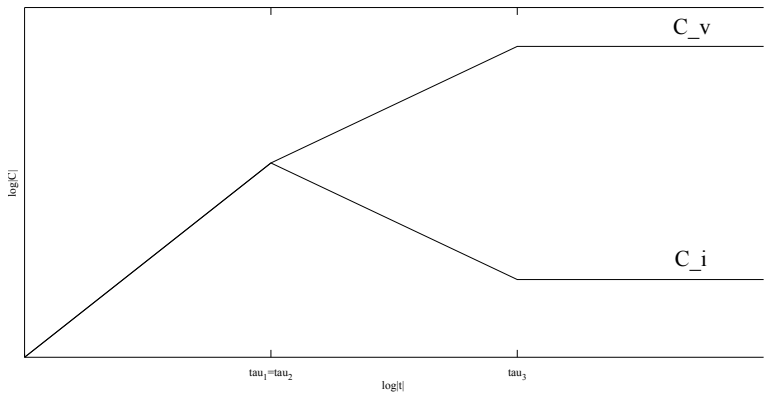

Figure 10: Low Temp Intermediate Sink Density Plot

10.4 Low Temp, High Sink Density

High Sink density causes interstitials to hit sinks before finding vacancies.
Initially

$$C_i = C_v = K_0t$$

$$\tau_2 = \frac{1}{K_{is}C_s}$$

Next C_i levels from sinks, C_v rises linearly

$$\frac{\partial C_i}{\partial t} = K_0 - K_{is}C_iC_s \approx 0$$

$$C_i = \frac{K_0}{K_{is}C_s}$$

$$C_v = K_0 t$$

at time τ_4 interstial loss from sinks equals loss to vacancies

$$K_{is}C_iC_s = K_{iv}C_iC_v \approx K_{iv}C_iK_0t$$

$$\tau_4 = \frac{K_{is}C_s}{K_{iv}K_0}$$

$$C_v = \left(\frac{K_0K_{is}C_st}{K_{iv}}\right)^{1/2}$$

$$C_i = \left(\frac{K_0}{K_{is}K_{iv}C_st}\right)^{1/2}$$

Steady state is reached at the same time and concentration formula except that C_s cannot be ignored

$$\tau_3 = \frac{1}{K_{vs}C_s}$$

$$C_v = \left(\frac{K_0K_{is}}{K_{iv}K_{vs}} + \frac{K_{is}^2C_s^2}{4K_{iv}^2}\right)^{1/2} - \frac{K_{is}C_s}{2K_{iv}}$$

$$C_v = \left(\frac{K_0K_{vs}}{K_{iv}K_{is}} + \frac{K_{vs}^2C_s^2}{4K_{iv}^2}\right)^{1/2} - \frac{K_{vs}C_s}{2K_{iv}}$$

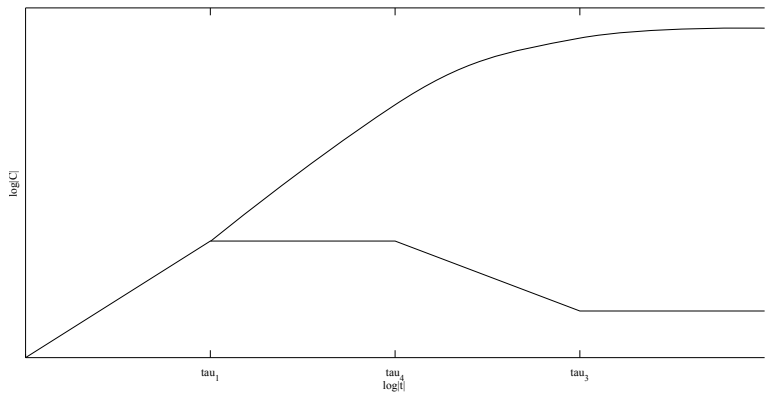

Figure 11: Low Temperature High Sink Density Plot

10.5 High Temperature Diffusion

At high temp, interstitials move to sinks quickly for recombination to occur so rate equations are:

$$\frac{\partial C_v}{\partial t} = K_0 - K_{vs} C_v C_s$$

$$\frac{\partial C_i}{\partial t} = K_0 - K_{is} C_i C_s$$

Initially

$$C_v = C_i = K_0 t$$

Next intersitials hit sinks at $\tau_2 = \frac{1}{K_{is} C_s}$

$$C_v = K_0 t$$

$$\frac{\partial C_i}{\partial t} = 0 = K_0 - K_{is} C_i C_s$$

$$C_i = \frac{K_0}{K_{is} C_s}$$

later vacancies hit sinks at $\tau_3 = \frac{1}{K_{vs} C_s}$

$$\frac{\partial C_v}{\partial t} = 0 = K_0 - K_{vs} C_v C_s$$

$$C_v = \frac{K_0}{K_{vs} C_s}$$

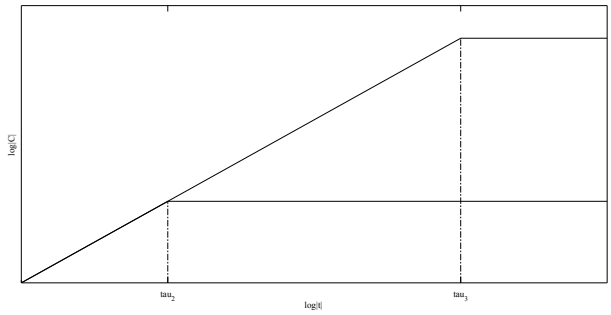

Figure 12: High Temperature Diffusion Plot

11 Swelling

Swelling is influence by temperature, dose, dose rate, composition, transmutation gas, and sink strength. Voids grow by collecting vacancies

$$\frac{\Delta V}{V} = \frac{4}{3} \pi r_c^3 N_c$$

Dose and Temperature Effects

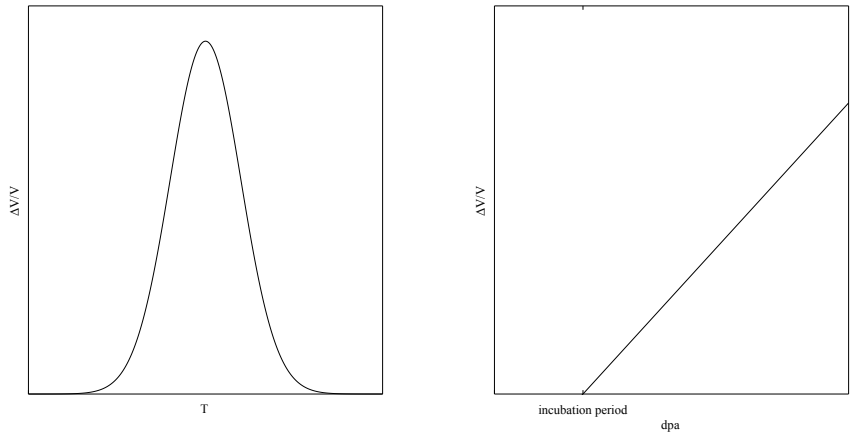

Figure 13: Dose and Temperature Effects Plots

Most metals swell in the range of $0.3T_m < T < 0.55T_m$
Austenitic steels

$$\frac{\Delta V}{V} \approx \frac{1\%}{dpa}$$

Dose Dependence

$$\frac{\Delta V}{V} \approx \frac{dose\,in\,dpa}{4}$$

Dose Rate Dependence
Peak Swelling temperature location depends on dose rate, sink strength, and defect loss mode.

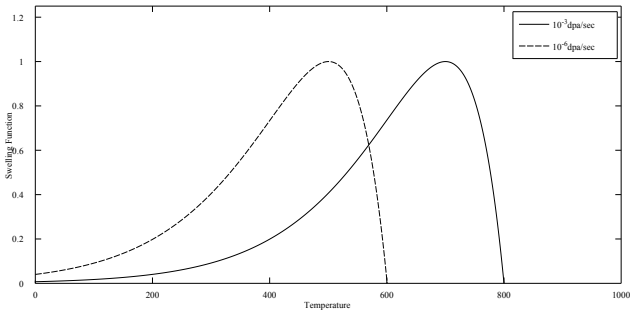

Figure 14: Dose Rate Shifting with the Peak Swelling Temperature

Dose rate effects the peak temperature increasing the dose rate also increases the incubation period.

Stress dependence

- the thermal emission term is the void growth factor effected by stress.
- stress at high temperatures can increase void growth rate if the stress is greater than the surface tension of the voids.

Radiation induced segregation

- RIS occurs at sinks with voids
- The shell of the sink changes in chemical composition which affects the void capture efficiency

Production Bias The size distribution of voids is dose dependent.

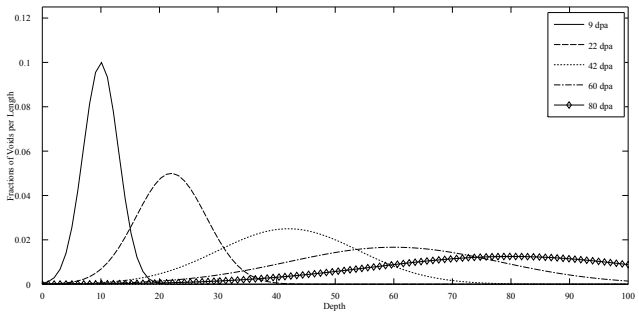

Figure 15: Fraction of Voids vs. Depth

12 Irradiation Creep

- Creep is time dependent deformation under an applied load and generall occurs at high temperature.
- Creep is different from swelling in that the material comlume is maintained in creep
- Creep does not occur if $T < \frac{1}{3}T_m$
- Creep failure occurs form long exposure below yield stress
- Creep failure occurs in 3 stages

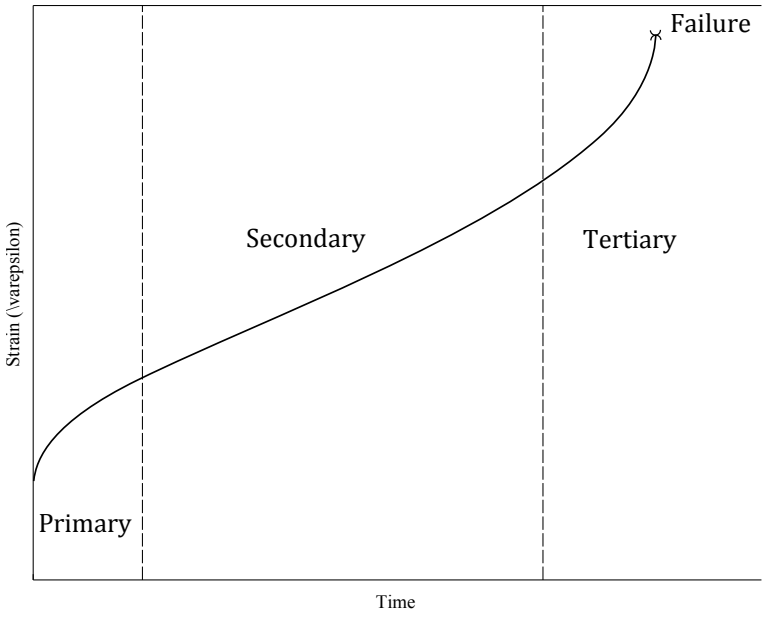

Figure 16: Strain vs. Time

1. Transient Strain rate decreases with time
2. Steady State
3. Tertiary Creep with recrystallization leads to cracks and voids

12.1 Mechanisms

Dislocations overcome barrier by thermal activation

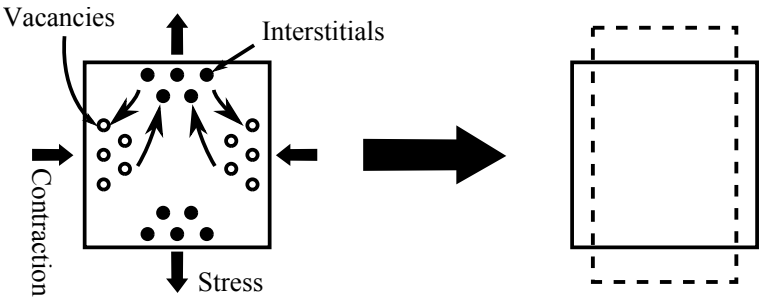

Figure 17: Diffusion Creep Diagrams

Grain Boundary Creep:

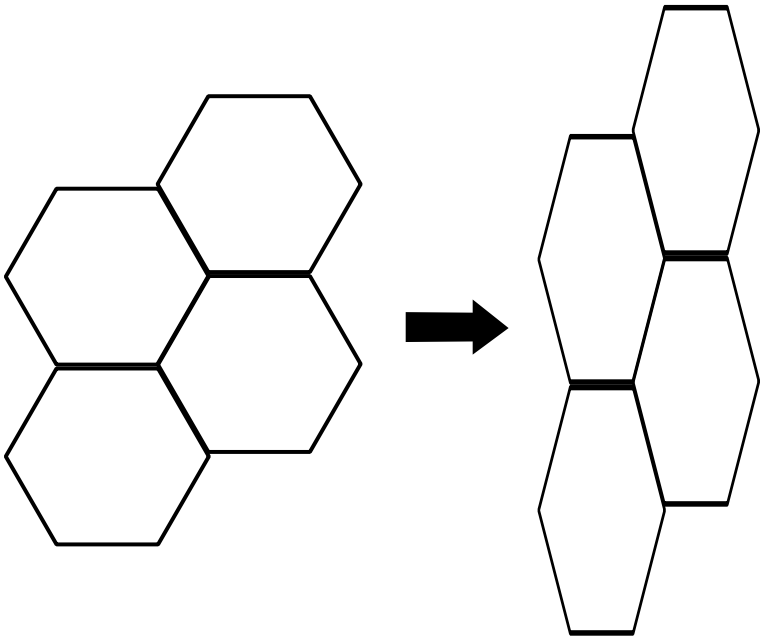

Figure 18: Grain Boundary Creep Diagrams

Table 2: Creep Mechanism Table

Mechanism	Favored by	Description
Nabarro-Herring	high temperature, low stress, large grains	vacancy diffusion through crystal
Coble	low stress, fine grains, temperature lower than N-H	vacancy diffusion along grain boundary
Grain Bound Sliding	same as N-H and Coble	sliding along with diffusion
Dislocation	high stress, low temperature, large grains	dislocation with climb over obstacles

13 Hardening

13.1 Radiation Hardening

Loss of ductility is the conern.

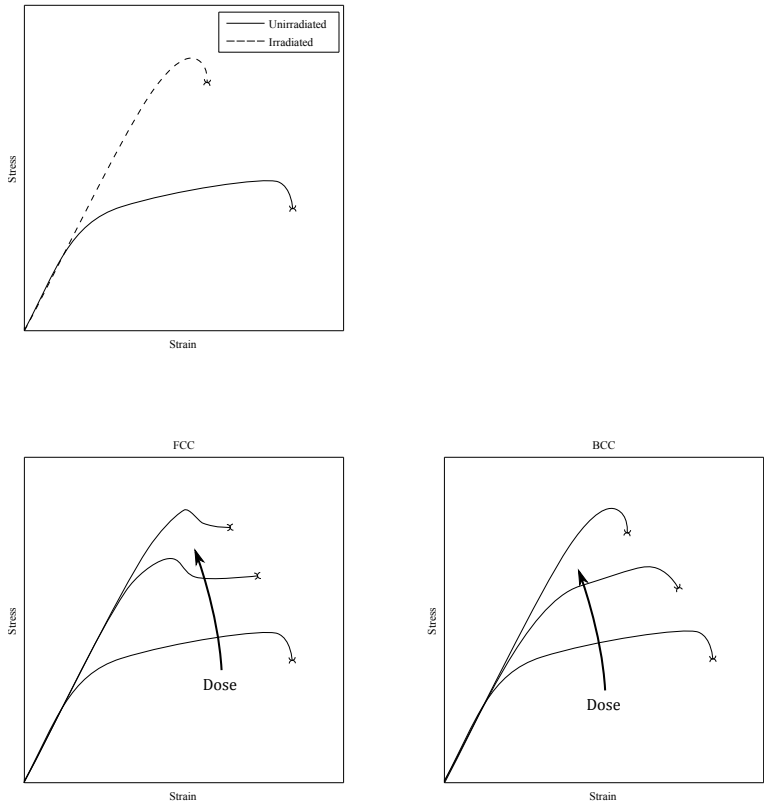

Figure 19: Loss of Ductility Plots

13.2 Mechanisms of Hardening

1. Increase stress needed to start dislocation motion (source Hardening)
2. Imede dislocation motion (friction hardening)

13.3 Defects by neutron radiation

- Point defects (very small effect)
- Impurity atoms (very small effect)
- vacancy clusters
- dislocation loops
- dislocation lines
- cavities
- precipitates

13.4 Frank Read Dislocation Source

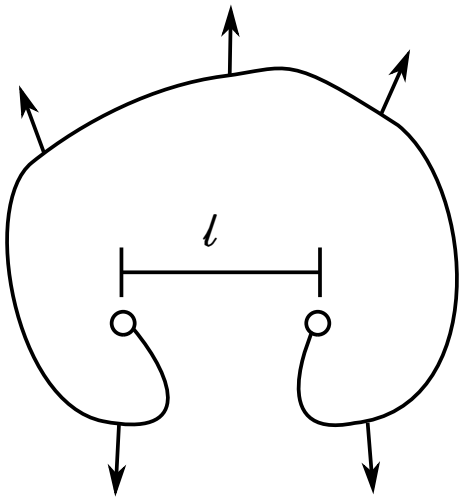

Figure 20: Frank Read Disloation Source

$$\sigma_s = \frac{Gb}{l}$$

13.5 Friction Hardening

- Resistance to motion by obstacles
  - clusters
  - loops
  - precipitates
  - voids
- Characterized by long range or short range
  - long range caused by dislocation-dislocation interactions
  - short range caused by discrete obstacles

$$\sigma_{Fr} = \sigma_{short} + \sigma_{long}$$

$$\sigma_{short} = \sigma_{precipitate} + \sigma_{void} + \sigma_{loops}$$

$$\sigma_{long} = \frac{Gb}{2\pi\sqrt{3}}\sqrt{\rho_{dislocation}}$$

14 Types of Fracture

- Ductile - Plastic deformation prior to failure
- Brittle - rapid crack propogation

ductility measured by Charpy Test (dropping hammer on hard surface)

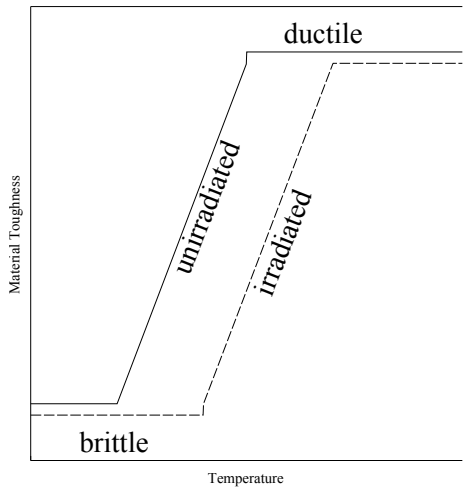

Figure 21: Transition from Brittle to Ductile Plot

Radiation changes the ductile to brittle transition temp (DBTT)

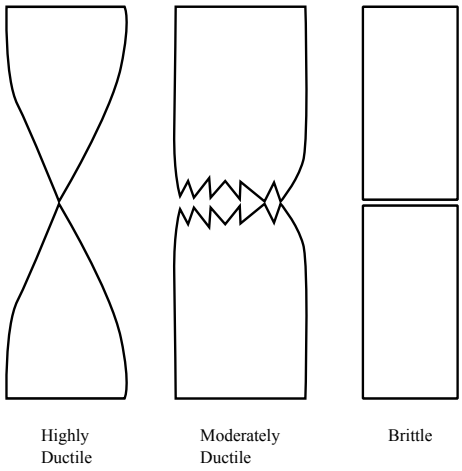

Figure 22: Failure Modes Diagram and Dimensional Changes Design Window Plot